IEEE Open Journal of
Power Electronics

Received 28 June 2024; revised 30 July 2024; accepted 3 August 2024. Date of publication 8 August 2024;
date of current version 15 August 2024. The review of this article was arranged by Associate Editor Hang Zhao.

Digital Object Identifier 10.1109/OJPEL.2024.3439593

Design Automation Using Exclusion-Based Hierarchical Computation for Power Electronics Converters in Harsh Environments

YUDI XIAO [1], ZHE ZHANG [2] (Senior Member, IEEE), GABRIEL ZSURZSAN [3] (Member, IEEE), MICHAEL A.E. ANDERSEN [3] (Member, IEEE), MARTIN MACFADYEN [1], YUCHUAN LIAO [1] (Graduate Student Member, IEEE), RAFAEL PENA ALZOLA [1] (Member, IEEE), WEIJIA YUAN [1] (Member, IEEE), AND MIN ZHANG [1] (Member, IEEE)

[1]Department of Electronic and Electrical Engineering, University of Strathclyde, G1 1XQ Glasgow, U.K.
[2]School of Electrical Engineering, Hebei University of Technology, Tianjin 300130, China
[3]Department of Electrical and Photonics Engineering, Technical University of Denmark, DK-2800 Kongens Lyngby, Denmark

CORRESPONDING AUTHOR: YUDI XIAO (e-mail: yudi.xiao@strath.ac.uk).

This work was supported in part by Innovation Fund Denmark (IFD) under Grant 8053-00095B and in part by UKRI Frontier Research Guarantee Grant EP/Y006437/1.

ABSTRACT Designing power electronics converters for harsh environments is challenging due to the absence of components' performance under harsh conditions, the frequent transition and data-passing among various software, and the time-consuming and computationally heavy work flow. This paper promotes using design automation to address the aforementioned design challenges. The implementations include public-accessible component databases, automated co-action among circuit simulators and finite element simulations to perform electrical, electromagnetic and thermal co-design, and finally an exclusion-based work flow with hierarchical computation to reduce computational load. The theorized framework is exemplified on designing a real world 175 °C 1.5 kW Three-level Neutral-point-clamped dc-dc converter. A database containing the high-temperature characteristics of SiC MOSFETs and ferrites is established and shared through a web application with graphical user interface. In 310 min, the program, which includes computationally heavy 3D finite element simulation, delivers design output after evaluating the converter's electrical, electromagnetic and thermal performance under 10 million parameter sets. Finally, a 1.5 kW dc-dc converter prototype is built and tested in 175 °C ambient temperature to verify the quality of the design output.

INDEX TERMS Application programming interface, component database, design automation, design methodology, extreme temperature.

NOMENCLATURE

Abbreviations

API	Application Programming Interface.
DAPE	Design Automation for Power Electronics.
FEMM	Finite Element Method Magnetics.
GUI	Graphical User Interface.
IC	Integrated Circuit.
MOSFET	Metal-oxide-semiconductor Field-effect Transistor.
PCB	Printed Circuit Board.
RMS	Root Mean Square.
SiC	Silicon Carbide.
TLNPC	Three-level Neutral-point-clamped.
ZVS	Zero Voltage Switching.

Symbols

D_p, D_s	Primary and secondary winding trace clearance.

f_s	Switching frequency.
L_{ac1}, L_{ac2}	Ac inductances.
L_f	Output inductance.
N_B	Number of interleaving layers of transformer.
T_R	Primary-to-secondary turns ratio of transformer.
V_{cp}	Clamping voltage of snubber.
W_p, W_s	Primary and secondary winding trace width.

I. INTRODUCTION

Designing a power electronics converter for harsh environments poses significantly greater challenges compared to designing for room environmental conditions with the same specifications. [1], [2]. Components exposed to harsh environments such as high or low temperature and strong radiation exhibit excessive parameter drifts. For example, the permeability of ferrite cores at cryogenic temperature (lower than −123 °C) can reduce to 10%∼50% of its nominal values at 25 °C [3]. The on-resistance of Silicon Carbide (SiC) Metal-oxide-semiconductor Field-effect Transistors (MOSFETs) exhibits up to a five-fold rise when the ambient temperature is increased from 25 °C to 225 °C [4]. Gate drivers can experience up to 27% change of latency, i.e., rise time, fall time, turn-on/off propagation delays, when exposed to a total ionizing dose of 1000 Gy ∼ 3000 Gy [5]. Conventional component- and circuit-models for room conditions need to be upgraded with extra parametrization. Moreover, since the interdependence between component behavior and circuit performance can be strong, harsh environment converter design involves both component- and system-level designs. For instance, Fig. 1 gives the dominant parametric drifts in extreme temperature environments and highlights the necessary co-action of software to correctly predict converter performance. Under a certain ambient temperature, the parametric changes of power semiconductor devices and Integrated Circuits (ICs) are firstly characterized, then modeled in spice simulators such as LTspice. Afterwards, the simulated node voltage and branch current are utilized as stimuli for electromagnetic simulation of magnetic components in finite element software such as COMSOL or Finite Element Method Magnetics (FEMM). The simulated loss of individual components are eventually used for obtaining temperature rise, which is fed back to correct the operating temperature of components. Such a routine is repeated until the temperature rise converges. The entire work flow requires consistent passing of data among different design software, which would be a tedious task for the designers. Furthermore, due to the extra parametrization in modeling components, and the combination of multiple software, the computation throughout the work flow is usually time-consuming [2].

The previously presented difficulties of designing a converter for harsh environments can be summarized as: the absence of component performance in harsh environments, the frequent transition and data-passing among software, and the time-consuming computation of work flow. All of these difficulties align with the challenges which design automation aims to address. As concluded in the second Design Automation for Power Electronics (DAPE) workshop, future research about design automation in the field of power electronics need to concentrate on improving availability of component data, standardizing Application Programming Interface (API) for easy co-action among different software, and finally paradigmatic change of work flow to reduce the complexity of the design process [6]. Therefore, design automation is potentially a solution to address all the difficulties of designing a converter for harsh environments.

The idea of design automation is not new in the field of power electronics. Automated routing of Printed Circuit Board (PCB) tracks have been a built-in function of many PCB design software for over 30 years [7], [8]. Automated optimization of the ac inductor in a phase-shifted full-bridge converter [9], automated topology selection based on specifications of power conversion [10], even an automated netlist generation tool has been available since the 2000s [11]. These early works of design automation in power electronics either utilize analytical equations, or reside in one software only. Cross-software implementations of design automation did not exist. Besides, a component database had not yet been established, and the evaluation of converter performance thereby lacked accuracy. In the past ten years, more and more researches dedicate to establishing a component-database, realizing co-action of different design software, and exploring efficient work flow of converter design. Component-databases are released either solely as raw data [12], or as web applications with Graphical User Interface (GUI) such as the MagNet Database from Princeton University [13]. Software co-action has been progressively realized as well. For instance, PowerSynth, which is developed by the University of Arkansas, enables automated multi-physics design of power modules for an optimized electrical thermal and mechanical performance. [14], [15], [16], [17], [18]. The work flow used for converter design have been mainly based on a methodology of optimization, whose block diagram is sketched in Fig. 2 [19], [20], [21], [22]. As shown, the circuit-level parameters (listed in parametric setting, such as switching frequency, modulation scheme and cooling methods, etc. [21]) and the component-level (e.g., selection of semiconductor devices [19], design of magnetic components [19], sizing of cold-plates [21]) are optimized separately. In the beginning, a global optimizer initializes a number of random trial solutions for the circuit-level parameters. A local optimizer then searches through libraries or databases for the selection component-level parameters, that gives the best converter performances (for example the minimum total loss [19], or the lightest converter weight [21]) under current circuit-level parameters. Once the local optimizations for all of the circuit-level parameters are completed, the global optimizer looks through the best converter performances that can be achieved by each set of the circuit-level parameters, and decides the variation of which for next global iteration. The entire optimization stops when the global optimizer thinks that the converter performances cannot be further improved, i.e., Pareto front has been found (as shown in the

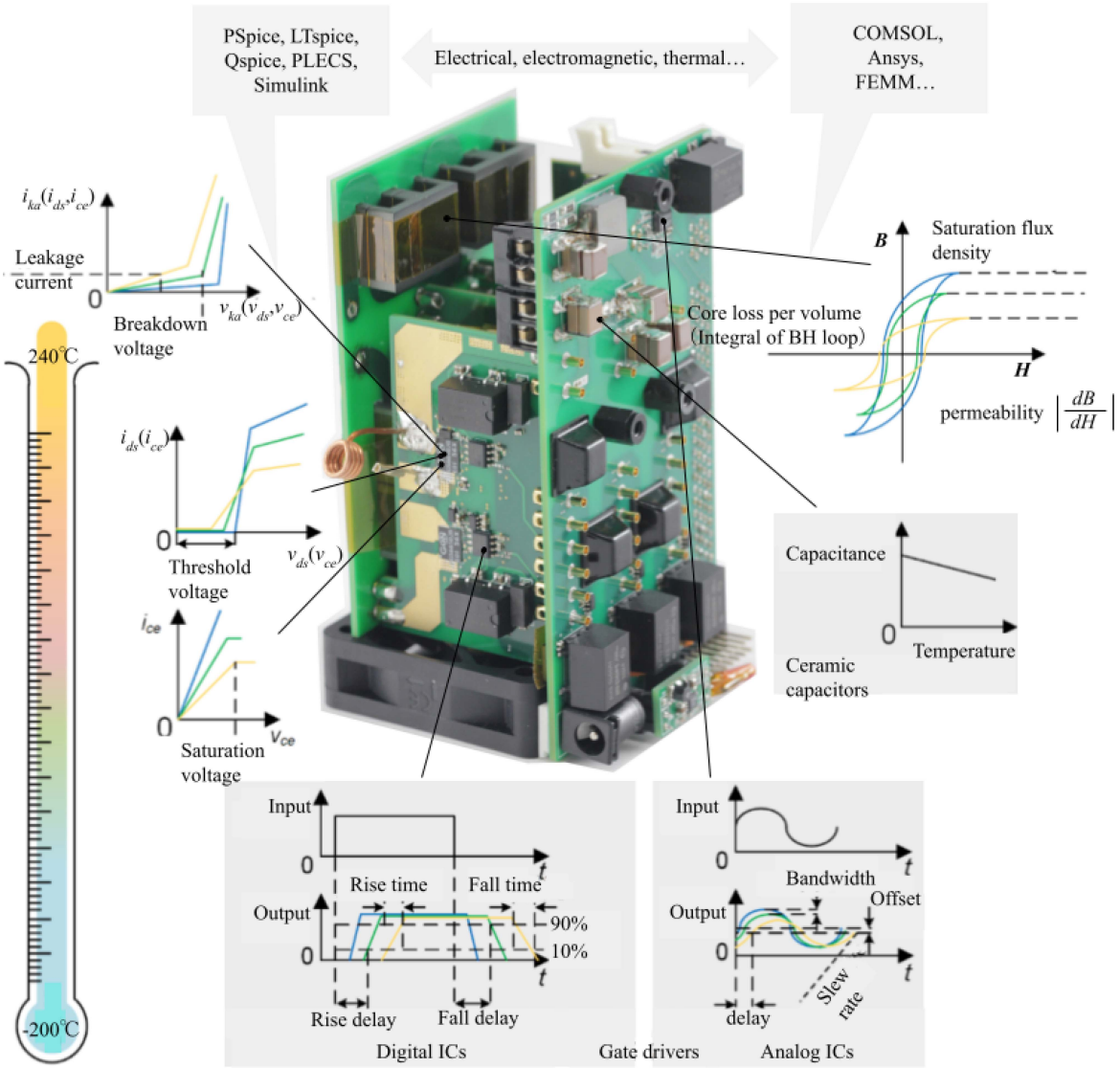

FIGURE 1. Example of components' parametric drifts in extreme temperature environments and the co-action of software for converter design.

'Output' area of Fig. 2). The features of the work flow universally adopted in literature (i.e., the one sketched in Fig. 2) are:

1) The methodology is optimizing for the best design.
2) Use cost functions to combine multiple design objectives into one.
3) Run through the same calculation in all iterations. Consequently, numerical simulations, which take longer time to execute than analytical models, are usually not used in the work flow.

This paper advances design automation in the field of power electronics, and uses the established design automation to address the three challenges of designing converters for harsh environments. Specifically, a web application is developed to share data from component characterizations under harsh conditions; circuit simulations and finite element analysis of components' electromagnetic and thermal performance are automated and combined using software APIs; an exclusion-based hierarchical work flow is proposed to include numerical analysis into the automated flow without provoking an overall heavy computational load. After this introduction, Section II presents the exclusion-based work flow. In contrast to an optimizing-based methodology, which optimizes for the best of one combined cost function, the exclusion-based filters out the disqualified ones with equal respect to judgements from every design objectives. Section III presents a case study, where the proposed work flow is applied step-by-step to a 1.5 kW Three-level Neutral-point-clamped (TLNPC) dc-dc converter specified for operating under 175 °C ambient temperature. A web application with GUI is developed to share data obtained from characterizing SiC MOSFETs and ferrite materials at 25 °C∼225 °C. Circuit simulator, FEMM and COMSOL are integrated through *MATLAB* script environment to automatically perform electrical, electromagnetic and thermal co-design. In 310 min, the program, which includes computationally heavy 3D finite element simulation, delivers design output after evaluating the converter's electrical, electromagnetic and thermal performance under 10 million

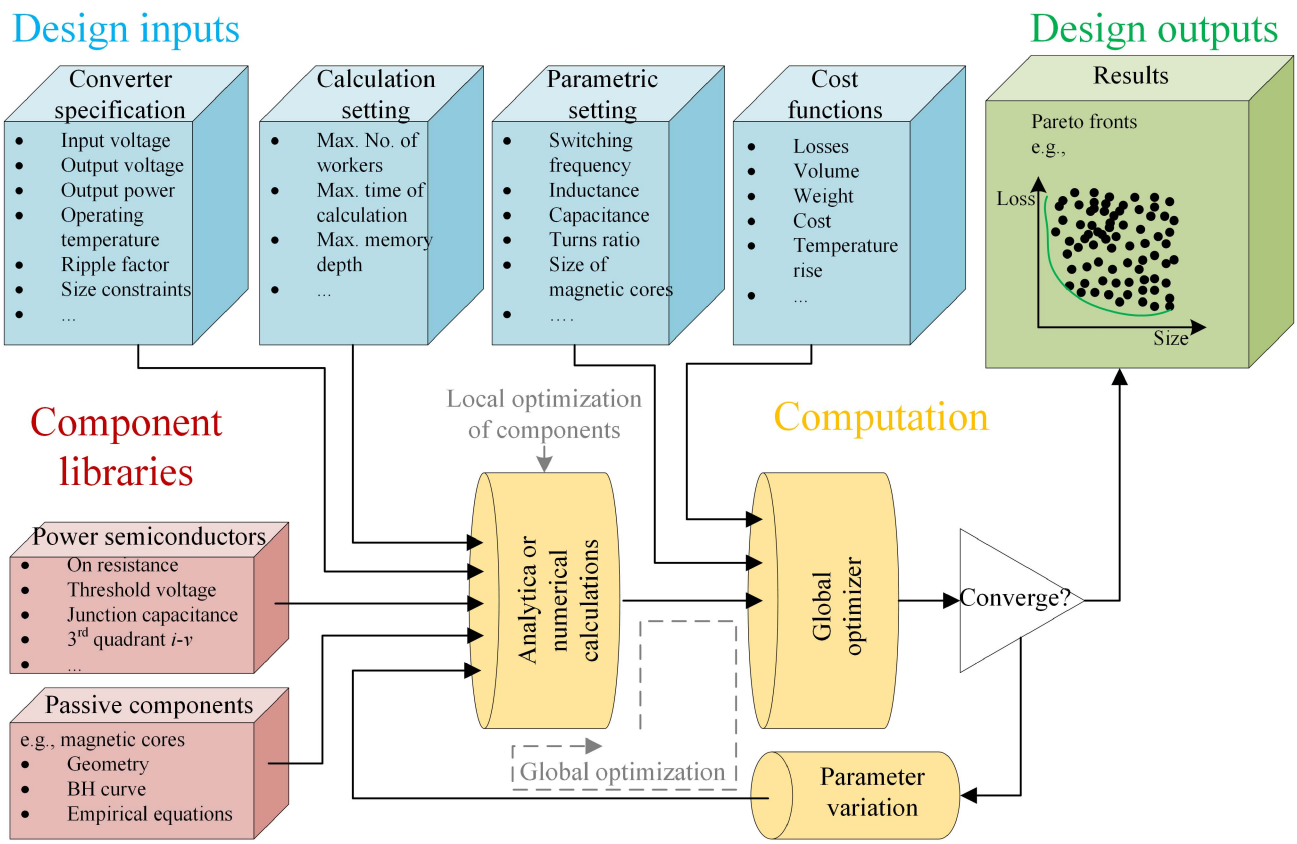

FIGURE 2. Block diagram of the design flow used in literatures about automatic converter design, i.e., [19], [20], [21], [22].

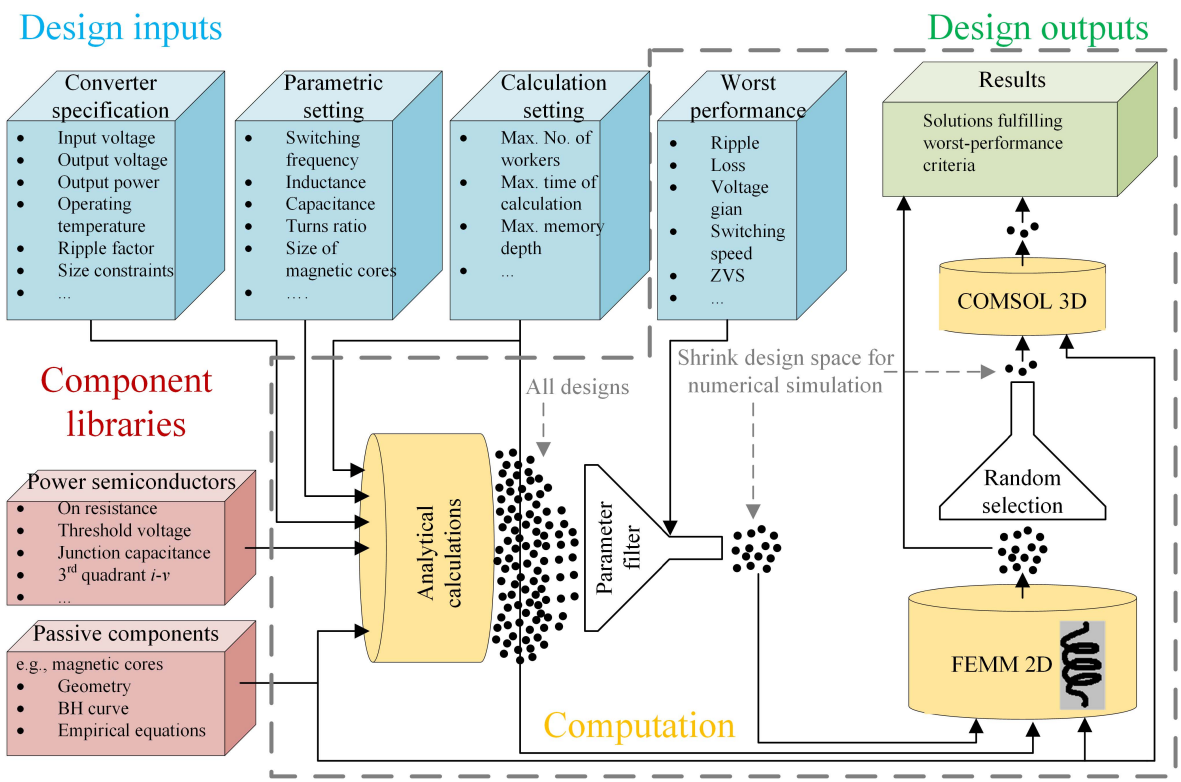

FIGURE 3. Block diagram of the exclusion-based hierarchical work flow (changes in regards to Fig. 2 are enclosed by the grey dashed lines).

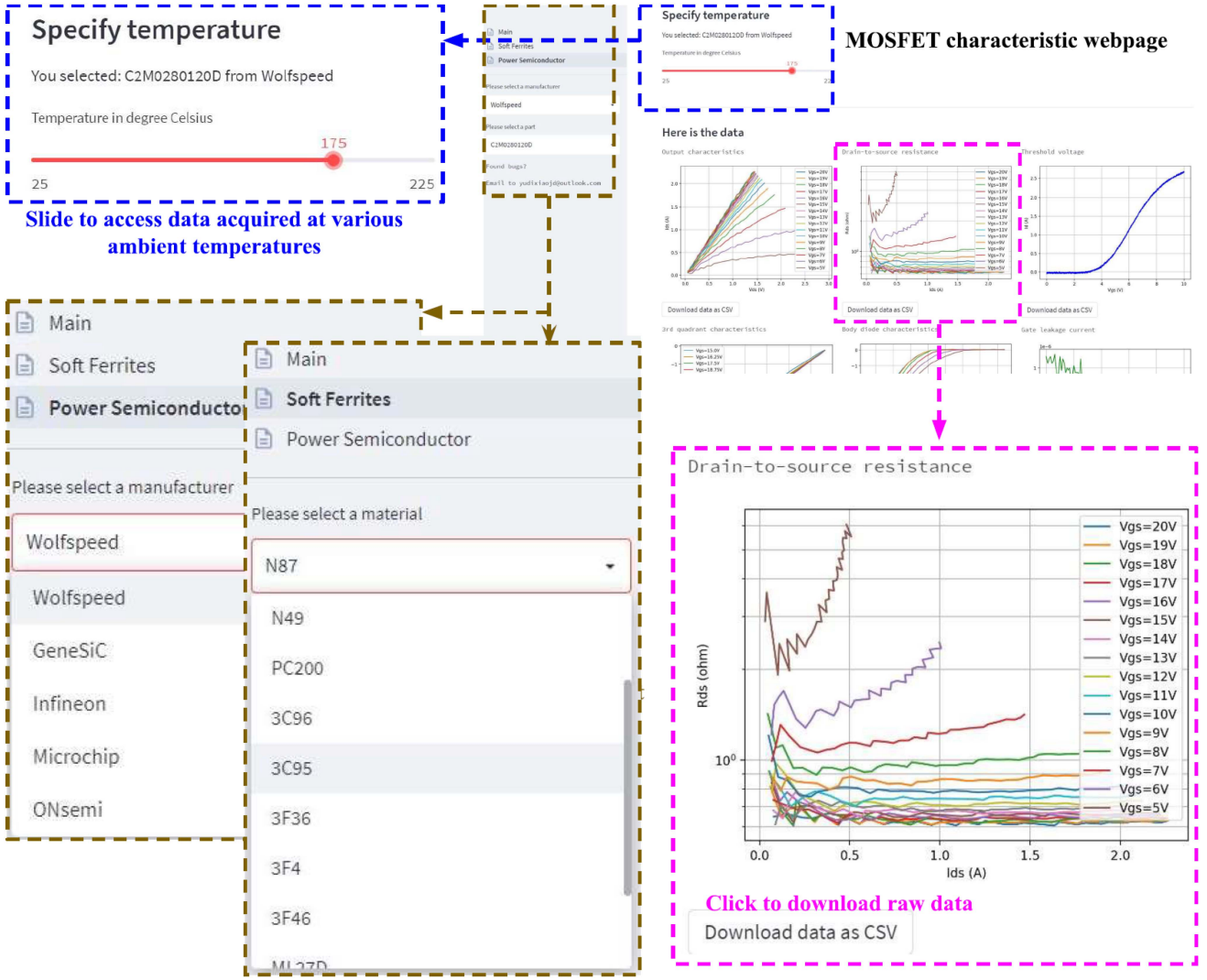

FIGURE 4. Screenshots of the developed web application for data sharing.

parameter sets. Finally, a 1.5 kW dc-dc converter prototype is built and tested in 175 °C ambient temperature to verify the quality of the design output. Section IV concludes this paper.

II. THE EXCLUSION-BASED HIERARCHICAL WORK FLOW

Fig. 3 sketches the block diagram of the exclusion-based hierarchical work flow. It differs from that of the method illustrated in Fig. 2 as described:

1) No optimizer was used. The design methodology is not optimizing for the best. Instead it filters out the disqualified ones.
2) No cost function was used. Multiple design criteria are set. Failure to meet any one of them disqualifies the parameter set.
3) Computations are arranged in hierarchies according to computational complexity. Parameter sets disqualified in a low-complexity hierarchy will not go through high-complexity computations.

Accordingly, the advantages of the proposed work flow over the prevalence are:

1) Does not require design of optimizer.
2) Does not need formulation of cost function. All criteria have physical meanings.
3) Overall computational complexity is reduced.

As shown in Fig. 3, the computation part is completely re-structured. There are three main hierarchies, i.e., the first with analytical calculations, the second with 2D numerical simulations, and the third with 3D numerical simulations. The computations of each main hierarchy can be further hierarchized. For example, in the analytical-calculation hierarchy, the computational load of estimating switching speed can be hundreds times heavier then that of calculating voltage gain of a converter (although both are usually much lighter than a 2D numerical simulation). For that reason, estimations of voltage gain and switching speed should be put into different local hierarchies, and be executed orderly. Implemented between adjacent hierarchies is a filter that checks the results from the

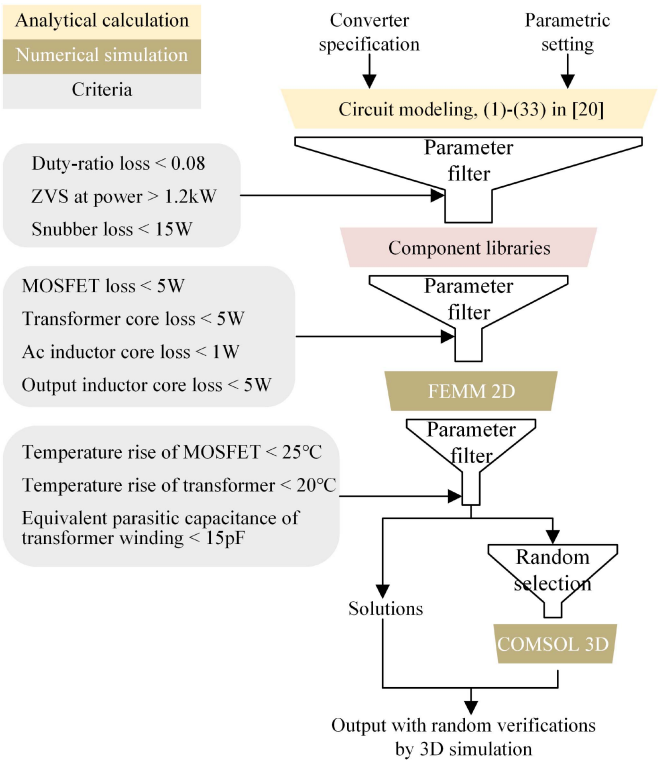

FIGURE 5. Block diagram of the hierarchical computation implemented in the case study.

previous hierarchy, and pass the qualified parameter sets to the next hierarchy.

The remaining changes are relatively small. The 'Cost functions' block in Fig. 2 is replaced by criteria defining the converter's worst allowed performances, such as ripple current/voltage, total loss, temperature rise, switching speed, volume. The output is no longer the best achievable performance (Pareto front) as in Fig. 2. Instead, it is the solutions that fulfill all of the defined criteria.

III. CASE STUDY:DESIGN AUTOMATION OF A THREE-LEVEL NEUTRAL-POINT-CLAMPED DC-DC CONVERTER

In this section, an example of implementing the proposed work flow (Fig. 3) is given. The script is written in *MATLAB*. The script is available for downloading from the link given in [23]. The target is to design an 1.2 kV-input 600V-output Three-level Neutral-point-clamped dc-dc converter with 3 kW rated power. Additionally, the converter is required to operate in an ambient temperature of 150 °C.

A. DEFINE INPUT

The converter specification has been defined, i.e., 1.2 kV input voltage, 600 V output voltage, 3 kW rated power and 150 °C operating temperature. Additionally, there are certain limitations on the form of prototype. Details of the specifications of the converter can be found in [24].

The parameters that need to be determined include six on the circuit level, i.e., switching frequency f_s (100 kHz ∼400 kHz with 50 kHz step size), two ac inductance L_{ac1} and L_{ac2} (each of 1 μ H∼ 6μH with 0.5 μH step size), turns ratio of transformer T_R (primary-to-secondary 0.5, 0.625 and 0.75), clamping voltage of output snubber V_{cp} (700 V, 800 V and 900 V), and output inductance L_f (80 μH∼160 μH with 20 μH step size); and a few component-level parameters, i.e., selection of powder cores for the output inductor, ferrite materials for the transformer and the ac inductors, and the geometric parameters of transformer winding (number of interleaving layers N_B, primary winding width W_p, primary winding clearance D_p, secondary winding width W_s and secondary winding clearance D_s). The switches (in this case MOSFETs) are excluded from the parameters of the design flow, because they are directly selected based on current rating, drain-to-source breakdown voltage and gate-to-source capacitance.

The worst case performances are defined with regards to duty-ratio loss (less than 0.08) and Zero Voltage Switching (ZVS) realization of the converter (achieve ZVS at power level above 1.2 kW), snubber loss (less than 15 W), loss and temperature rise of each power MOSFET (less than 4 W and 25 °C, respectively), loss and case temperature of the transformer (less than 10 W and 20 °C, respectively), loss of each ac inductor (less than 2 W), loss of the output inductor (less than 10 W), and parasitic capacitance of transformer winding (less than 15 pF). Analytical modeling of ZVS realization of the converter can be found in [24].

B. ESTABLISH COMPONENT LIBRARIES

The converter is specified to operate under an ambient temperature of 150 °C, where the components' behavior can have significant changes from that at room temperature. Therefore, libraries of critical components must contain these temperature drift characteristics. Considering 50 °C∼75 °C of temperature rise due to self-heating of components, this design requires libraries that specify component characteristics at 200 °C∼225 °C. Such component databases are absent at present, and hence, have to be built from scratch.

Therefore, on resistance, threshold voltage, gate-to-source and drain-to-source leakage current, and junction capacitances of a few commercially available SiC power MOSFETs, as well as *BH* curves of a few commercially available ferrite materials are characterized at 25 °C∼225 °C ambient temperature. The acquired data is then used to build up the two libraries shown in Fig. 3, i.e., the MOSFET and the core library. Powder cores have relatively high *Curie* temperature (400 °C∼700 °C) compared to ferrite materials (below 260 °C), and hence, are less critical in high temperature converter design. For this reason, a temperature-independent library for powder cores published by *Magnetics Inc* is directly used, as part of the core library in Fig. 3.

Using *Streamlit*, we have developed a web application with GUI to share the component data obtained from high-temperature characterization. Fig. 4 gives a screenshot of the

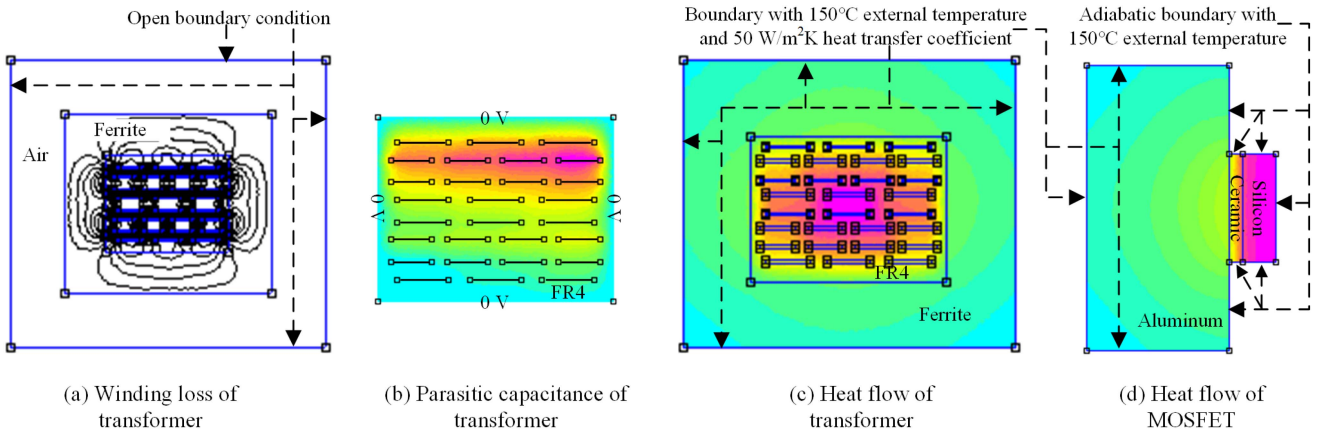

(a) Winding loss of transformer (b) Parasitic capacitance of transformer (c) Heat flow of transformer (d) Heat flow of MOSFET

FIGURE 6. **Model settings and boundary conditions of the *FEMM* 2D simulations, i.e., the third-hierarchy computation, in the case study (So far the script to interface *FEMM* is only able to automatically draw E-shape cores and planar conductors in planar 2D problems).**

web application. The aforementioned component characteristics acquired under 25 °C∼225 °C ambient temperature are not only visualized, but also made available for downloading. The web application can be accessed through the link given in [25].

C. HIERARCHIZE COMPUTATIONS

Fig. 5 visualizes the implemented hierarchical computation. In total there are four hierarchies, i.e., two for analytical calculations, one for 2D numerical simulations, and the last one for 3D numerical simulations. The calculations in the top three hierarchies are executed in parallel by fifteen workers.

The first hierarchy uses analytical equations, which have been published in [26], to estimate circuit-level behavior of the TLNPC dc-dc converter. After the calculations of this hierarchy, the parameter sets are justified by the circuit-level criteria, i.e., duty-ratio loss, ZVS realization and losses in snubber circuit. The search space is squeezed before starting calculations in the second hierarchy.

The first-hierarchy calculations also output the converters' waveforms, among which the critical ones are the current through the MOSFETs, the current through and the voltage across the transformer, the ac inductors and the output inductor. These critical waveforms are then used in the second hierarchy to calculate the conduction loss of the MOSFETs and the loss of the magnetic components. The calculation of the MOSFET loss is simply based on the Root Mean Square (*RMS*) value of the MOSFET current and the on resistance of the MOSFETs under current ambient temperature. The winding loss of the magnetic components are estimated under an assumption that the current is distributed evenly in copper with 4 A/mm^2 density. The core loss of the magnetic components are estimated using the Steinmetz's equation, where the coefficients are extracted from the core library, and the maximum flux density and the frequency are determined by the frequency spectrum of the volatge waveform obtained from the first-hierarchy calculations. After the second-hierarchy analytical calculations, parameter sets that lead to excessive loss in the MOSFETs and the magnetic components are excluded.

The third-hierarchy refines the modeling of winding loss in the previous hierarchy. Additionally, it estimates the case temperature of the MOSFETs and the transformer, and the parasitic capacitance of the transformer winding. *FEMM* is used to carry out the simulations [27]. The design flow interfaces with the *FEMM* software by its API to *MATLAB*. The geometric settings and the boundary conditions of the *FEMM* simulations are summarized in Fig. 6. As shown, all simulations are planar 2D problems. In the transformer simulations, the window area that is not occupied by conductors is assumed to be filled with FR4 material. In the electrostatic simulation of the transformer, the planar conductors are simplified as line segments. In the heat flow simulation of the MOSFETs, a heat sink with dimension of 21 mm × 42 mm is attached to the MOSFET with 2mm-thick thermal interface material in between. The exposed segments of the MOSFET and the thermal interface material, and the segment of the heat sink that is attached by the thermal interface material, are assumed to be adiabatic. After the third-hierarchy *FEMM* simulations, parameter sets that result in overheating of the transformer or the MOSFETs, or lead to excessive parasitic capacitance in the transformer winding are excluded.

The last hierarchy, i.e., the fourth, carries out 3D FEM simulations to check the accuracy of winding loss modeling in the *FEMM* 2D simulations in the previous hierarchy. In this case study, the parameter set that gives the minimum transformer winding loss according to the *FEMM* simulations is picked out for 3D verification. *COMSOL Multiphysics* is used, and is interfaced through one of its APIs called *LiveLink*^{TM} *for MATLAB*. Fig. 7 shows the transformer 3D model that is automatically draw by the program.

D. OUTPUT OF THE CASE STUDY

Fig. 8 visualizes the problem size and the computing time of each of the four computational hierarchies of the case study. In total there are 9676800 parameter sets that need to be evaluated. The first-hierarchy computation filtered out

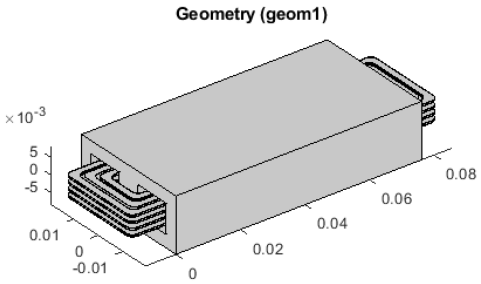

FIGURE 7. 3D model of transformer automatically created in the case study (So far the script to interface *COMSOL* is only able to automatically draw E-shape cores with planar conductors and toroid cores with round wires).

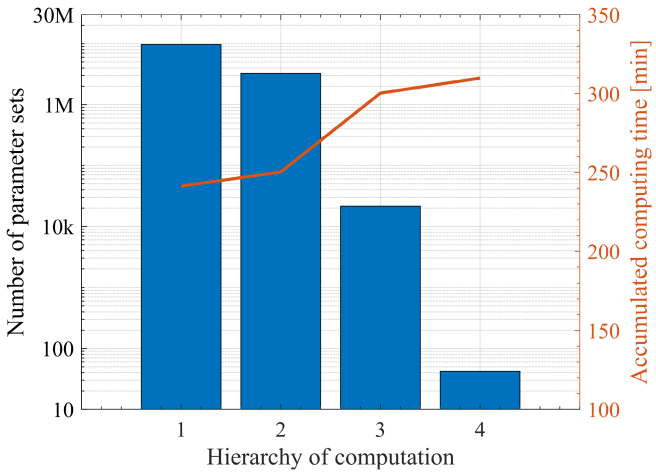

FIGURE 8. Problem size and computing time of each of the four hierarchies in the case study.

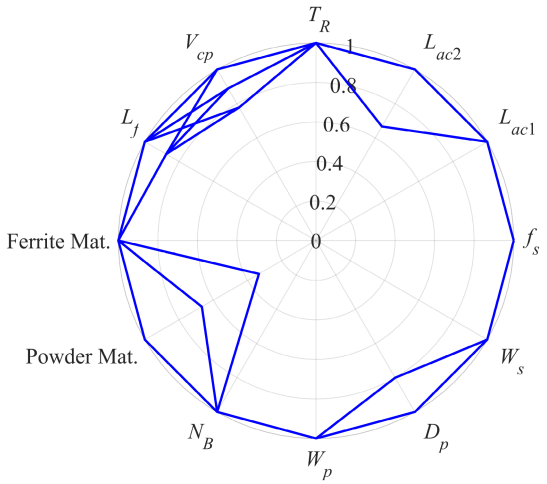

FIGURE 9. The 42 solutions of the design flow (Each polygon outline represents one solution. Value of parameters are unified with regards to the maximum). Abbreviation: Mat.-material.

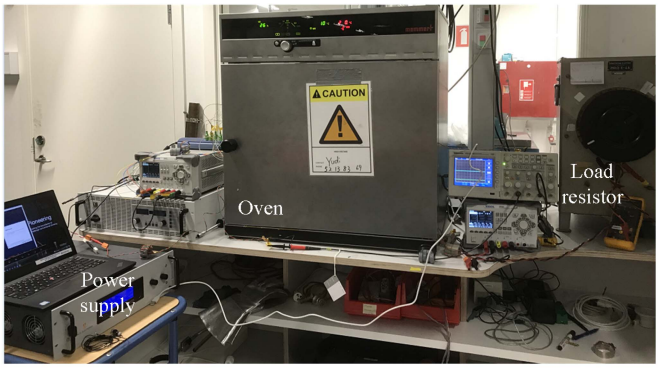

(a) Setup for high-temperature test of the TLNPC prototype

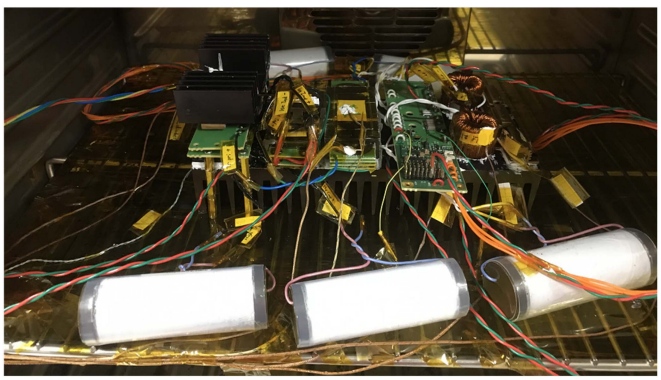

(b) TLNPC prototype inside of oven

FIGURE 10. Test setup of the designed TLNPC dc-dc converter.

two thirds of them. The second hierarchy evaluated 3251200 parameter sets, and passed 21504 of them to the third. In the end, 42 parameter sets remained and were fed to output. One of the 42 was picked out for validation of winding loss by 3D FEM simulations. The entire DA program was executed on a *PowerEdge R740 Rack Server* (installed with two Intel Xeon Gold 6148 processors) from *DELL*. With 15 workers running in parallel, the total computing time is 310 min.

Fig. 9 gives the 42 solutions recommended by the design flow. As shown, they are distinguished by slight variations the clamping voltage, the output inductance, the clearance of transformer primary winding, and a large difference in the second ac inductance, and the powder core material. It should be noted that although being different solutions, they all fulfill the design criteria specified in Section III-A. A final solution is selected considering availability and lead time of powder cores.

The winding loss from *COMSOL* 3D simulation is 2.7 times of that from *FEMM* 2D. Using the winding loss from 3D simulation, the case temperature of the transformer core is estimated to be up to 200 °C. Therefore, the thermal design of the transformer may need adjustments, such as increasing convective heat transfer from the core to environment, or implementing direct heat transfer from the winding to environment.

A TLNPC dc-dc converter prototype was built according to the design output. The prototype was tested at ambient temperature up to 175 °C. Fig. 10 shows the test setup and the prototype. The case temperatures of the transformer core, the transformer winding and one of the four MOSFETs were

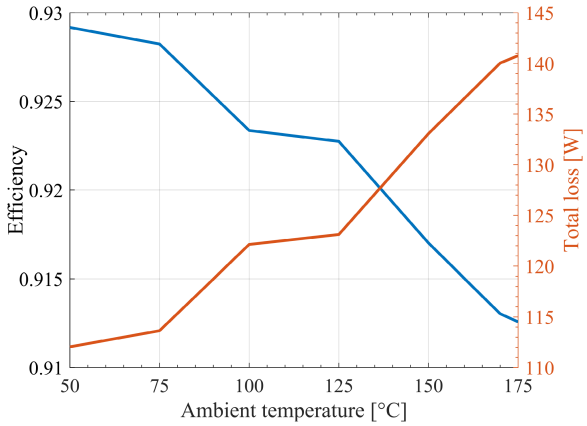

FIGURE 11. Measured efficiency and total loss of the TLNPC prototype over ambient temperature @ 1kV-input voltage, 600V-output voltage and 1.5kW-output power.

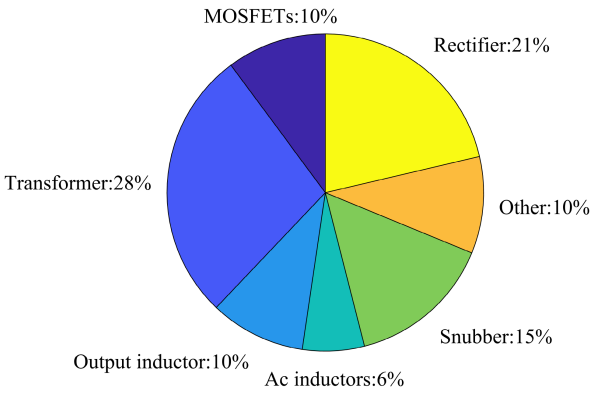

FIGURE 12. Estimated loss breakdown of the prototype @ 1kV-input voltage, 600V-output voltage, 1.5kW-output power, and 175 °C ambient temperature.

sensed by K-type thermocouples. The input of the prototype was connected to a *SM1500* DC power supply from Delta-Elektronika. The output of the prototype was connected to a 250 Ω load resistor. The input voltage and current were read from the front panel of *SM1500*. The output voltage and current were measured through *FLUKE 175* multi-meters.

Fig. 11 plots the measured efficiency and loss of the prototype over ambient temperature. As shown, the efficiency drops with temperature. The total loss of the converter increases by 27% at 175 °C ambient temperature with reference to that at 50 °C. Fig. 12 gives the estimated loss breakdown of the prototype running at 175 °C ambient temperature. As shown, the transformer contributes the highest loss among the components. In spite of that, such a relatively high loss is the actually the lowest that can be achieved under the criteria of keeping the parasitic capacitance of the transformer winding below 15 pF. If, for example, the criteria of parasitic capacitance is loosened to 39 pF, the minimum transformer winding loss could theoretically be halved. In this design, to ensure functional operation of the converter, the criteria of parasitic capacitance was kept at 15 pF. Consequently, the transformer was overheated. Fig. 13 shows the case temperature of the

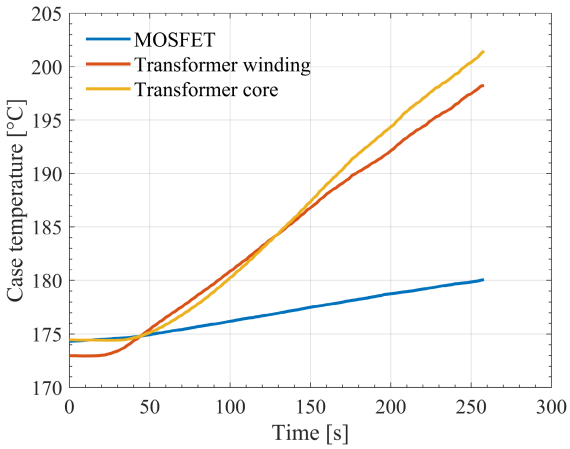

FIGURE 13. Measured case temperature of the MOSFET, the transformer winding and the transformer core @ 1kV-input voltage, 600V-output voltage, 1.5kW-output power, and 175 °C ambient temperature (Test was stopped at 250 s time cap as the transformer core reached 200 °C).

MOSFETs, the transformer winding, and the transformer core, respectively. The MOSFETs did not overheat. However, the temperature rise of the transformer quickly reached 25 °C. The issue of transformer overheating will be addressed with improved cooling methods, such as encapsulating the transformer in thermally conductive compound.

IV. CONCLUSION

This paper promotes using design automation in the field of power electronics. Obtained component characteristics should be established as public accessible databases, as well as the scripts manipulating the co-action among different design software. The current methodology of optimizing in converter design has a drawback of fuzzing the judgement of individual criterion. Incorporating a methodology of exclusion, which equally respects the judgements from all the criteria, could help reduce computational load. However, an obvious disadvantage of the proposed exclusion-based methodology is that it does not produce the best achievable outcome of each design objective as the optimization-based methodology does. Therefore, the two methodologies differ in capabilities and are suitable for different design scenarios:

1) The optimization-based methodology overlooks the entire design space and glimpses the limit of every design objective. Its computation encompasses a large (relative to the exclusion-based option) number of iterations, and usually chooses analytical component- and circuit models to limit the overall computational load. To ensure a correct estimation of the converter performance, the analytical models have to be accurate. Therefore, the optimization-based methodology is suitable for design cases where the behaviours of circuits and components are well studied and have been analytically modeled.
2) The exclusion-based methodology abandons a fraction of the design space immediately if the fraction fails to meet any one of the design criteria. Whether or not the

remaining criteria are satisfied in the abandoned fraction is not estimated. The reduced number of computational routines allows the exclusion-based methodology to use complicated component- and circuit-models. Therefore, the exclusion-based methodology is suitable for design cases where either the component- or the circuit-models are computationally heavy.

This paper proposes that converter design for harsh environments, where the computational load is heavy due to the high complexity of component models and the frequent data-passing among software, will especially benefit from design automation with the exclusion-based methodology. To prove this claim, an 175 °C 1.5 kW Three-level Neutral-point-clamped dc-dc converter is designed using design automation. A database containing the high-temperature characteristics of SiC MOSFETs and ferrites is published through a self-developed web application. An exclusion-based work flow is built to realize the design automation. In 310 min, the program, which includes computationally heavy 3D finite element simulation, delivers design output after evaluating the converter's electrical, electromagnetic and thermal performance under 10 million parameter sets. Finally, a 1.5 kW dc-dc converter prototype is built and tested in 175 °C ambient temperature to verify the quality of the design output.

REFERENCES

[1] J. Watson and G. Castro, "A review of high-temperature electronics technology and applications," *J. Mater. Sci.: Mater. Electron.*, vol. 26, pp. 9226–9235, 2015.

[2] Y. Xiao, Z. Zhang, M. S. Duraij, T. -G. Zsurzsan, and M. A. E. Andersen, "Review of high-temperature power electronics converters," *IEEE Trans. Power Electron.*, vol. 37, no. 12, pp. 14831–14849, Dec. 2022.

[3] S. Yin et al., "Characterization of inductor magnetic cores for cryogenic applications," in *2021 IEEE Energy Convers. Congr. Expo.*, Vancouver, BC, Canada, 2021, pp. 5327–5333, doi: 10.1109/ECCE47101.2021.9595353.

[4] Z. Gu et al., "Comparative study on high-temperature electrical properties of 1.2 kV SiC MOSFET and JBS-integrated MOSFET," *IEEE Trans. Power Electron.*, vol. 39, no. 4, pp. 4187–4201, Apr. 2024, doi: 10.1109/TPEL.2023.3338487.

[5] R. Lai et al., "A radiation-hard gate driver circuit for high voltage application," in *2020 32nd Int. Symp. Power Semicond. Devices ICs*, Vienna, Austria, 2020, pp. 262–265, doi: 10.1109/ISPSD46842.2020.9170061.

[6] K. Hermanns, Y. Peng, and A. Mantooth, "The increasing role of design automation in power electronics: Gathering what is needed," *IEEE Power Electron. Mag.*, vol. 7, no. 1, pp. 46–50, Mar. 2020.

[7] T. Hubing, P. Grover, T. V. Doren, J. Drewniak, and L. Hill, "An algorithm for automated printed circuit board layout and routing evaluation," in *1993 Int. Symp. Electromagn. Compat.*, 1993, pp. 318–321, doi: 10.1109/ISEMC.1993.473720.

[8] Y. Fukumoto, S. Miura, H. Ikeda, T. Nakayama, S. Tanimoto, and H. Uemura, "A method of automatic placement that reduces electromagnetic radiation noise from digital printed circuit boards," in *Proc. IEEE Int. Symp. Electromagn. Compat. Symp. Rec.*, 2000, vol. 1, pp. 363–368, doi: 10.1109/ISEMC.2000.875594.

[9] P. Wallmeier, N. Frohleke, and H. Grotstollen, "Automated optimization of high frequency inductors," in *Proc. 24th Annu. Conf. IEEE Ind. Electron. Soc.*, 1998, vol. 1, pp. 342–347, doi: 10.1109/IECON.1998.724147.

[10] B. Omrane, N. Mariun, I. B. Aris, S. M. Bashi, and S. Taib, "Expert system-based approach to automate the design process of power electronics converters," in *Proc. IEEE/PES Transmiss. Distrib. Conf. Exhib.*, 2002, vol. 3, pp. 1943–1946, doi: 10.1109/TDC.2002.1177756.

[11] Y. Usami, Y. Inagaki, M. Nakahara, and K. Harada, "An automated design system for switching power regulators," in *Proc. 25th Int. Telecommun. Energy Conf.*, 2003, pp. 334–339.

[12] F. Tian, D. B. Cobaleda, and W. Martinez, "Automatic data extraction based on semiconductor datasheet for design automation of power converters," in *2022 Int. Power Electron. Conf.*, Himeji, Japan, 2022, pp. 922–927, doi: 10.23919/IPEC-Himeji2022-ECCE53331.2022.9806859.

[13] H. Li, D. Serrano, S. Wang, and M. Chen, "MagNet-AI: Neural network as datasheet for magnetics modeling and material recommendation," *IEEE Trans. Power Electron.*, vol. 38, no. 12, pp. 15854–15869, Dec. 2023, doi: 10.1109/TPEL.2023.3309233.

[14] N. Hingora, X. Liu, Y. Feng, B. McPherson, and A. Mantooth, "Power-CAD: A novel methodology for design, analysis and optimization of power electronic module layouts," in *2010 IEEE Energy Convers. Congr. Expo.*, 2010, pp. 2692–2699, doi: 10.1109/ECCE.2010.5618043.

[15] T. M. Evans et al., "PowerSynth: A power module layout generation tool," *IEEE Trans. Power Electron.*, vol. 34, no. 6, pp. 5063–5078, Jun. 2019, doi: 10.1109/TPEL.2018.2870346.

[16] I. A. Razi, Q. Le, H. A. Mantooth, and Y. Peng, "Physical design automation for high-density 3D power module layout synthesis and optimization," in *2020 IEEE Energy Convers. Congr. Expo.*, 2020, pp. 1984–1991, doi: 10.1109/ECCE44975.2020.9235982.

[17] T. M. Evans, S. Mukherjee, Y. Peng, and H. A. Mantooth, "Electronic design automation (EDA) tools and considerations for electro-thermo-mechanical co-design of high voltage power modules," in *2020 IEEE Energy Convers. Congr. Expo.*, Detroit, MI, USA, 2020, pp. 5046–5052, doi: 10.1109/ECCE44975.2020.9235818.

[18] I. Al Razi, Q. Le, T. M. Evans, H. A. Mantooth, and Y. Peng, "PowerSynth 2: Physical design automation for high-density 3-D multichip power modules," *IEEE Trans. Power Electron.*, vol. 38, no. 4, pp. 4698–4713, Apr. 2023, doi: 10.1109/TPEL.2022.3227300.

[19] T. B. Soeiro, J. Mühlethaler, J. Linnér, P. Ranstad, and J. W. Kolar, "Automated design of a high-power high-frequency LCC resonant converter for electrostatic precipitators," *IEEE Trans. Ind. Electron.*, vol. 60, no. 11, pp. 4805–4819, Nov. 2013, doi: 10.1109/TIE.2012.2227897.

[20] M. S. Mohammed and R. A. Vural, "Evolutionary design automation of high efficiency series resonant converter for photovoltaic systems," *IEEE Trans. Power Electron.*, vol. 35, no. 11, pp. 11332–11343, Nov. 2020, doi: 10.1109/TPEL.2020.2987086.

[21] Z. Dong, R. Ren, F. Wang, and R. Chen, "An automated design tool for three-phase motor drives," in *2021 IEEE Des. Methodol. Conf.*, 2021, pp. 1–6, doi: 10.1109/DMC51747.2021.9529944.

[22] Q. Yang and M. Steurer, "An automated optimal design procedure of a nonlinear inductor-based hybrid DC circuit breaker," in *2023 IEEE Des. Methodologies Conf.*, Miami, FL, USA, 2023, pp. 1–6, doi: 10.1109/DMC58182.2023.10412508.

[23] Y. Xiao, "AutoPE case study," GitHub.com. Accessed, Aug. 2024. [Online]. Available: https://github.com/YudiXiao/AutoPE_case_study

[24] Y. Xiao, M. S. Duraij, Z. Zhang, T. -G. Zsurzsan, and M. A. E. Andersen, "ZVS design in Full-SiC three-level neutral-point-clamped DC–DC converter considering quasi-linear output capacitance C_{oss}," *IEEE Trans. Ind. Electron.*, vol. 70, no. 9, pp. 8970–8978, Sep. 2023, doi: 10.1109/TIE.2022.3206704.

[25] Y. Xiao, "Data from my PhD," Streamlit.io. Accessed, Aug. 2024. [Online]. Available: https://yudiphddata.streamlit.app/Power_Semiconductor

[26] Y. Xiao, M. Duraij, Z. Zhang, G. Zsurzsan, M. Hansen, and B. Thomsen, "Design automation combining analytical models and numerical simulations for three-level neutral-point-clamped DC-DC converter," in *2021 IEEE Des. Methodol. Conf.*, 2021, pp. 1–6, doi: 10.1109/DMC51747.2021.9529930.

[27] "Finite element method magnetics," 2004. [Online]. Available: https://www.femm.info/wiki/HomePage